

Generation of pulse trains in the normal dispersion regime of a dielectric medium with a relaxing nonlinearity

Jose M. SotoCrespo and Ewan M. Wright

Citation: *Appl. Phys. Lett.* **59**, 2489 (1991); doi: 10.1063/1.105983

View online: <http://dx.doi.org/10.1063/1.105983>

View Table of Contents: <http://apl.aip.org/resource/1/APPLAB/v59/i20>

Published by the [American Institute of Physics](http://www.aip.org).

Related Articles

Switching of bound vector solitons for the coupled nonlinear Schrödinger equations with nonhomogeneously stochastic perturbations

Chaos **22**, 043132 (2012)

Metamaterial features in a dielectric fiber with an inserted thin cylindrical shell

Appl. Phys. Lett. **101**, 143508 (2012)

Simple visible supercontinuum light source with true continuous-wave output power

Appl. Phys. Lett. **101**, 091112 (2012)

Dependences of Brillouin frequency shift on strain and temperature in optical fibers doped with rare-earth ions

J. Appl. Phys. **112**, 043109 (2012)

Hidden possibilities in controlling optical soliton in fiber guided doped resonant medium

AIP Advances **1**, 022137 (2011)

Additional information on *Appl. Phys. Lett.*

Journal Homepage: <http://apl.aip.org/>

Journal Information: http://apl.aip.org/about/about_the_journal

Top downloads: http://apl.aip.org/features/most_downloaded

Information for Authors: <http://apl.aip.org/authors>

ADVERTISEMENT

JANIS Does your research require low temperatures? Contact Janis today.
Our engineers will assist you in choosing the best system for your application.



10 mK to 800 K
Cryocoolers
Dilution Refrigerator Systems
Micro-manipulated Probe Stations

LHe/LN₂ Cryostats
Magnet Systems

sales@janis.com www.janis.com
Click to view our product web page.

Generation of pulse trains in the normal dispersion regime of a dielectric medium with a relaxing nonlinearity

Jose M. Soto-Crespo and Ewan M. Wright

Optical Sciences Center, University of Arizona, Tucson, Arizona 85721

(Received 18 March 1991; accepted for publication 15 August 1991)

We show that modulation-type instability can occur in the normal dispersion regime of a dielectric medium for the case of a relaxing self-focusing nonlinearity. This instability leads to the generation of pulse trains with almost no pedestal when periodic boundary conditions are applied.

It is well known that the combination of linear group velocity dispersion (GVD) and self-phase modulation (SPM) as arises in optical fibers or other nonlinear dielectric media can give rise to a variety of soliton¹⁻⁴ and instability phenomena⁵⁻⁷ which are well described by the nonlinear Schrödinger equation (NLSE). In the anomalous dispersion regime, the NLSE has a family of bound-state multisoliton solutions,¹ which have been verified experimentally,² and modulation instability is also present.⁵⁻⁷ Modulation instability (MI) is a process by which the amplitude of a weak periodic perturbation on a continuous wave (cw) background can grow exponentially leading to a temporal modulation.⁸

In this letter we show that modulation-type instability can also occur in the normal dispersion regime of a dielectric medium for the case of a relaxing self-focusing nonlinearity. We use the name modulation-type instability since MI is usually reserved for that instability which occurs for an instantaneous response in the anomalous GVD regime.⁵⁻⁸ However, as we demonstrate, the present instability shows many of the features of the usual MI. This instability was previously predicted by Trillo *et al.*⁹ who referred to it as a Raman MI.⁹ It is well known that a relaxing nonlinearity provides an approximate model¹⁰ of the effects of stimulated Raman scattering (SRS) in silica-core fibers.^{10,11} Recently there has been considerable interest in understanding the effects of SRS on MI in the anomalous dispersion regime,¹²⁻¹⁶ and numerical results predict that it should be possible to generate pulse trains without the pedestal which appears for an instantaneously responding medium.^{6,16} We present numerical results which show that similar trains of pulses can be generated in the normal dispersion regime for a relaxing nonlinearity when periodic boundary conditions are imposed. In an analogous but distinct problem Fleck and Carman¹⁷ have previously shown that trains of pulses can also be generated during the spatial self-focusing of ultrashort pulses in a medium with a relaxing nonlinearity.

To investigate the effects of a relaxing nonlinearity we consider the following modified NLSE written in soliton units²

$$i \frac{\partial u}{\partial z} = \frac{\beta}{2} \frac{\partial^2 u}{\partial t^2} - \phi u, \quad (1)$$

where

$$t_R \frac{\partial \phi}{\partial t} = -\phi + |u|^2, \quad (2)$$

where u is the electric field envelope and ϕ is the nonlinear phase shift. The two terms on the right hand side of Eq. (1) describe the effects of GVD and nonlinear phase modulation, respectively, with $\beta = +1$ corresponding to normal GVD and $\beta = -1$ to anomalous GVD. Equation (2) accounts for the relaxing nature of the nonlinear phase shift ϕ , t_R being the dimensionless response time (if $t_R = 0$ Eqs. (1) and (2) reduce to the usual NLSE). The stability of the cw solutions ($\partial/\partial t = 0$) of Eqs. (1) and (2) can be investigated using a perturbed homogeneous solution of the form ($|\epsilon|, |\mu| \ll 1$)

$$u(t, z) = u_0 [1 + \epsilon e^{i(\Omega t + \delta z)} + \mu e^{(-i\Omega t + \delta^* z)}] e^{i|u_0|^2 z}, \quad (3)$$

where the right-most exponential factor accounts for the SPM due to the cw wave, Ω is the detuning of the sidebands ϵ and μ from the frequency of the cw field, and δ is generally a complex number. The side bands ϵ and μ correspond to the down-shifted Stokes field and the up-shifted anti-Stokes field components respectively ($\Omega > 0$). By substituting Eq. (3) into Eqs. (1) and (2) an eigenproblem results whose eigenvalues determine δ , and the corresponding eigenvectors yield ϵ and μ . These eigenvectors can be used to investigate the effects of Stokes anti-Stokes coupling,^{9,11,18} but here we concentrate on the eigenvalues. A straightforward calculation gives

$$\delta = \pm \frac{i\Omega}{2} \sqrt{\beta^2 \Omega^2 + \frac{4\beta|u_0|^2}{(1 + i\Omega t_R)}}, \quad (4)$$

and instability follows when $Re(\delta) > 0$. Figure 1(a) shows the growth rate $Re(\delta)$ as a function of scaled detuning Ω for $u_0 = 1$, $t_R = 0.05$, and both anomalous GVD (dashed line) and normal GVD (solid line). It is straightforward to show that in both cases the cw solution is unstable for all $\Omega > 0$ if the response time t_R is nonzero. For anomalous GVD the growth rate displays two maxima at $\Omega_{MI} \cong \sqrt{2}|u_0|$, and $\Omega_R \cong 1/t_R$. The first maximum Ω_{MI} corresponds to the usual MI (with some modification due to the finite response time), and the second occurs at the detuning Ω_R of peak Raman gain.^{9,11,14} In contrast, for normal GVD there is a single maximum at $\Omega \cong \Omega_R$.⁹

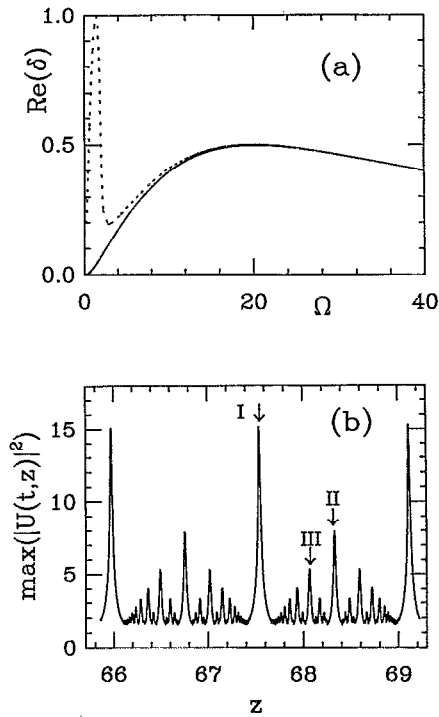


FIG. 1. (a) Growth rate $Re(\delta)$ as a function of scaled detuning Ω for $u_0 = 1$, $t_R = 0.05$, and both anomalous (dashed line) and normal (solid line) GVD, and (b) maximum value of $|u(t,z)|^2$ over the range $[0, t_{\max}]$ as a function of the propagation coordinate z .

We have solved Eqs. (1) and (2) using the split step Fourier method¹⁹ with periodic boundary conditions on the time interval $[0, t_{\max}]$, and the initial condition

$$u(t,0) = u_0 [1 + \epsilon(t) e^{i\Omega_R t}], \quad (5)$$

where $\epsilon(t)$ is the amplitude of the perturbation which has a mean detuning equal to that for peak Raman gain Ω_R . The amplitude $\epsilon(t)$ is assumed periodic with period t_{\max} , and this provides the natural time scale for the introduction of periodic boundary conditions. As is usual the split step method entails splitting the propagation into linear and nonlinear steps, and at each nonlinear step Eq. (2) is solved numerically, for a given intensity distribution $|u|^2$, using the fast Fourier transform which automatically imposes periodic boundary conditions.²⁰ The temporal grid size t_{\max} was chosen such that $\Omega_R t_{\max} = 2\pi m$, where m is an integer, and up to 512 temporal grid points were used. In the numerical algorithm the sampled frequencies are then integer multiples of Ω_R/m .²⁰ For the numerical calculations reported here we set $u_0 = 1$, $t_R = 0.05$ ($\Omega_R = 20$), $m = 10$ ($t_{\max} = \pi$), and $\epsilon(t) = A \exp[-B^2(t/t_{\max} - 1/2)^2]$, with $A = 10^{-3}$ and $B = 4$. (With these parameter values $\epsilon(0) \cong \epsilon(t_{\max}) \cong 0$ and $\epsilon(t)$ approximates a periodic perturbation.)

Figure 1(b) shows the periodic nature of the predicted instability in the normal GVD regime. Here we show the maximum value of $|u(t,z)|^2$ over the range $[0, t_{\max}]$ as a function of the propagation coordinate z . For the range of z values shown two oscillation periods are observed, but we remark that for increasing z , $\max(|u(t,z)|^2)$ slowly in-

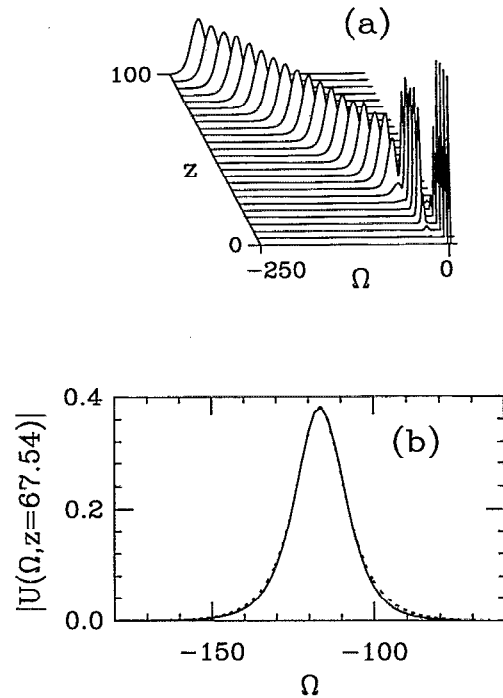


FIG. 2. (a) Evolution of the frequency spectrum $|u(\Omega,z)|$ corresponding to Fig. 1(b), where $u(\Omega,z)$ is the Fourier transform of $u(t,z)$, and (b) the frequency spectrum at $z = 67.54$ (solid line), along with the best fit hyperbolic secant profile (dashed line) which is characteristic of solitons in the anomalous GVD regime.

creases indicating that the oscillations are not perfectly periodic. Figure 2(a) shows the corresponding evolution of the frequency spectrum $|u(\Omega,z)|$, where $u(\Omega,z)$ is the Fourier transform of $u(t,z)$. After an initial transient the frequency spectrum settles down into a fixed profile whose mean frequency down-shifts at a nearly constant rate. Figure 2(b) shows this fixed profile at $z = 67.54$ (solid line), along with the best fit hyperbolic secant profile (dashed line) which is characteristic of solitons in the anomalous GVD regime. Clearly the frequency spectrum is tending towards a sech-like structure whose mean frequency down shifts due to the effects of SRS.

If it were the case that the frequency spectra shown in Fig. 2 also had at most a linear phase chirp in the frequency domain, then a sech-like profile would also arise in the temporal domain since the Fourier transform of a hyperbolic secant is itself a hyperbolic secant. However, this is only the case for those z values corresponding to the global maxima in Fig. 1(b). Figure 3(a) shows the temporal field profile at the point labeled I in Fig. 1(b). The dashed line Fig. 3(a) was obtained by taking the modulus of the Fourier transform of the corresponding frequency spectrum (dashed line) in Fig. 2(b). Therefore, for these propagation distances the initial cw field (plus perturbation) coheres into a temporal sech-like structure. At propagation distances corresponding to the other global maxima in Fig. 1(b) the temporal profile is the same as that in Fig. 3(a) except the pulse center is shifted due to the combined effects of SRS, which down-shifts the mean frequency, and GVD which in turn causes the pulse to move.

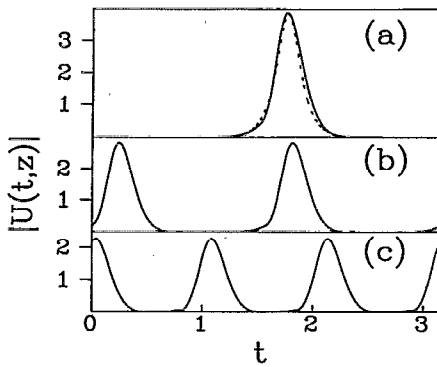


FIG. 3. Temporal field profiles $|u(t,z)|$ corresponding to the points labeled (a) I ($z = 67.54$), (b) II ($z = 68.325$), and (c) III ($z = 68.065$) in Fig. 1(b).

For general propagation distances the temporal field profiles are found to be very complicated. However, sech-like structures also appear for z values corresponding to the local maxima in Fig. 1(b). The temporal field profiles corresponding to the local maxima labeled II and III in Fig. 1(b) are shown in Figs. 3(b) and 3(c), respectively. Here we see the appearance of two and three sech-like structures. Inspection shows that for the case of two (three) structures the energy in each is one half (third) of that in Fig. 3(a), and that the individual field profiles in each case are almost identical. We also note that, in comparison to the usual MI, these pulse trains have a relatively small pedestal, even in Fig. 3(c).

Finally, an estimate of the generated pulse widths can be obtained by considering the dimensional Raman shift Δ_R defined by $\Delta_R T_s = \Omega_R$. Here T_s is the dimensional time unit which arises in the introduction of soliton units,² and $t = T/T_s$ where T is the dimensional time. By setting $\Delta_R = 13$ THz, which is the accepted value for fused silica,^{10,11} and $\Omega_R = 20$, we obtain $T_s \cong 2$ ps. Therefore, with reference to Fig. 3, the predicted pulse widths are of the order of ps. The required fiber lengths and peak powers required will depend on the specific value of the GVD parameter k_2 .²

In conclusion, we have shown that modulation-type instability can occur even in the normal dispersion regime of a dielectric medium for the case of a relaxing self-focusing nonlinearity. Although this instability is not a MI in the strict sense it displays many of the characteristics of an

MI, namely it causes an initial cw wave to undergo periodic oscillations and leads to the formation of sech-like structures. Furthermore, we have demonstrated the generation of pulse trains with variable number of pulses, and almost no pedestal, when periodic boundary conditions are applied.

This work was supported by the Joint Services Optical Program of the Air Force Office of Scientific Research and the Army Research Office, the Army Research Office (DAAL03-88-K0066), and J. M. Soto-Crespo acknowledges a grant from the Ministerio de Educaci3n y Ciencia, Spain. The authors would like to thank Dr. David R. Heatley for useful discussions, and a hardware donation from ATT is gratefully acknowledged.

- ¹ A. Hasegawa and F. Tappert, *Appl. Phys. Lett.* **23**, 142 (1973); **23**, 171 (1973).
- ² L. F. Mollenauer, R. H. Stolen, and J. P. Gordon, *Phys. Rev. Lett.* **45**, 1095 (1980).
- ³ D. Kr3kel, N. J. Halas, G. Giuliani, and D. Grischkowsky, *Phys. Rev. Lett.* **60**, 29 (1988).
- ⁴ A. M. Weiner, J. P. Heritage, R. J. Hawkins, R. N. Thurston, E. M. Kirschner, D. E. Leairdm, and W. J. Tomlinson, *Phys. Rev. Lett.* **61**, 2445 (1988).
- ⁵ A. Hasegawa and W. F. Brinkman, *IEEE J. Quant. Electron. Lett.* **16**, 694 (1980).
- ⁶ A. Hasegawa, *Opt. Lett.* **9**, 288 (1984).
- ⁷ K. Tai, A. Hasegawa, and A. Tomita, *Phys. Rev. Lett.* **56**, 135 (1986).
- ⁸ V. I. Bespalov and V. I. Talanov, *JETP Lett.* **3**, 307 (1966) [*Pis'ma Zh. Eksp. Teor. Fiz.* **3**, 471 (1966)]; T. B. Benjamin and J. E. Feir, *J. Fluid Mech.* **27**, 417 (1967).
- ⁹ S. Trillo, S. Wabnitz, G. I. Stegeman, and E. M. Wright, *J. Opt. Soc. Am. B* **6**, 889 (1989).
- ¹⁰ R. H. Stolen, J. P. Gordon, W. J. Tomlinson, and H. A. Haus, *J. Opt. Soc. Am. B* **6**, 1159 (1989).
- ¹¹ K. J. Blow and D. Wood, *IEEE J. Quant. Electron.* **25**, 2665 (1989).
- ¹² M. J. Potasek, *Opt. Lett.* **12**, 921 (1987).
- ¹³ M. N. Islam, S. P. Djaili, and J. P. Gordon, *Opt. Lett.* **13**, 518 (1988).
- ¹⁴ M. N. Islam, G. Sucha, I. Bar-Joseph, M. Wegener, J. P. Gordon, and D. S. Chemla, *J. Opt. Soc. Am. B* **6**, 1149 (1989).
- ¹⁵ E. Golovchenko, P. V. Mamyshev, A. N. Pilipetskii, E. M. Dianov, *IEEE J. Quant. Electron.* **26**, 1815 (1990).
- ¹⁶ P. V. Mamyshev, S. V. Chernikov, E. M. Dianov, and A. M. Prokhorov, *Opt. Lett.* **15**, 1365 (1990).
- ¹⁷ J. A. Fleck and R. L. Carman, *Appl. Phys. Lett.* **20**, 290 (1972).
- ¹⁸ See also N. Bloembergen, *Nonlinear Optics* (New York, Benjamin, 1965) p. 110.
- ¹⁹ J. A. Fleck, Jr., J. R. Morris, and M. D. Feit, *Appl. Phys.* **10**, 129 (1976).
- ²⁰ See, for example, W. H. Press, B. P. Flannery, S. A. Teukolsky, and W. T. Vetterling, *Numerical Recipes* (Cambridge University, Cambridge, 1986), Chap. 12.